Journal of Magnetic Resonance 212 (2011) 234–239

Contents lists available at ScienceDirect

Journal of Magnetic Resonance

journal homepage: www.elsevier.com/locate/jmr

Communication

Broadband excitation and indirect detection of nitrogen-14 in rotating solids using Delays Alternating with Nutation (DANTE)

Veronika Vitzthum [a], Marc A. Caporini [a,*], Simone Ulzega [a], Geoffrey Bodenhausen [a,b,c,d]

[a] Institut des Sciences et Ingénierie Chimiques, Ecole Polytechnique Fédérale de Lausanne, 1015 Lausanne, Switzerland
[b] Département de Chimie, Ecole Normale Supérieure, 24 rue Lhomond, 75005 Paris, France
[c] Université Pierre et Marie Curie, 75005 Paris, France
[d] CNRS, UMR 7203, 75005 Paris, France

ARTICLE INFO

Article history:
Received 13 May 2011
Revised 12 June 2011
Available online 20 July 2011

Keywords:
Nitrogen-14 NMR
Delays Alternating with Nutations for Tailored Excitation (DANTE)
Dipolar Heteronuclear Multiple-Quantum Correlation (D-HMQC)
Solid-state NMR
Magic angle spinning (MAS)
Broadband excitation
Quadrupolar nuclei

ABSTRACT

A train of short rotor-synchronized pulses in the manner of Delays Alternating with Nutations for Tailored Excitation (DANTE) applied to nitrogen-14 nuclei ($I = 1$) in samples spinning at the magic angle at high frequencies (typically $\nu_{rot} = 62.5$ kHz so that $\tau_{rot} = 16$ μs) allows one to achieve uniform excitation of a great number of spinning sidebands that arise from large first-order quadrupole interactions, as occur for aromatic nitrogen-14 nuclei in histidine. With routine *rf* amplitudes $\omega_1(^{14}N)/(2\pi) = 60$ kHz and very short pulses of a typical duration $0.5 < \tau_p < 2$ μs, efficient excitation can be achieved with 13 rotor-synchronized pulses in 13 $\tau_{rot} = 208$ μs. Alternatively, with 'overtone' DANTE sequences using 2, 4, or 8 pulses per rotor period one can achieve efficient broadband excitation in fewer rotor periods, typically 2–4 τ_{rot}. These principles can be combined with the indirect detection of ^{14}N nuclei via spy nuclei with $S = ½$ such as ^{1}H or ^{13}C in the manner of Dipolar Heteronuclear Multiple-Quantum Correlation (D-HMQC).

1. Introduction

Nitrogen plays structural and functional roles of fundamental importance in proteins and nucleic acids that are essential to many processes in living organisms. Nitrogen-14 is potentially an attractive spectroscopic probe because of its favorable isotopic abundance (99.6%) and reasonable gyromagnetic ratio (~70% of ^{15}N). However, ^{14}N NMR is not yet a well-established spectroscopic technique. Unlike nuclei with spin $S = 1/2$ such as ^{13}C and ^{15}N, ^{14}N has a spin $I = 1$ and a nuclear quadrupole moment Q. The interaction of ^{14}N nuclei with local electric field gradients is characterized by a quadrupole coupling constant C_Q which can be quite large. In static powders or crystals, this leads to spectra spanning several MHz that are difficult to excite uniformly and require probes and receivers with broad bandwidths, thus limiting the sensitivity. In solid-state NMR, the first-order components of second-rank tensor interactions (e.g., dipolar couplings, anisotropic chemical shifts and quadrupole interactions) can be averaged out by magic angle spinning (MAS). Nevertheless, even with very fast spinning ($\nu_{rot} > 50$ kHz), ^{14}N MAS NMR spectra are characterized by dozens of spinning sidebands [1], the envelope of which critically depends on several parameters [2]. Here we propose a new excitation method based on a DANTE scheme [3–6], where trains of short rotor-synchronized pulses (typically with $0.5 < \tau_p < 2$ μs) are used to excite ^{14}N coherences. We shall see that this allows one to excite very large families of spinning sidebands in a uniform manner. Recent work using frequency swept pulses [7] has shown broadband excitation in static solids, however these approaches are not efficient when combined with MAS.

It has been shown in recent years [8,9] that reliable ^{14}N spectra can be obtained through indirect detection via a spy nucleus (typically ^{1}H or ^{13}C) in the manner of heteronuclear single- and multiple-quantum correlation spectroscopy (HSQC and HMQC). The indirect detection of ^{14}N exploits the transfer of coherence between single- or double-quantum (SQ or DQ) nitrogen-14 coherences and SQ coherences of suitable spy nuclei with spin $S = 1/2$ such as ^{1}H or ^{13}C, as described in detail elsewhere [2,8–15]. So far, these methods have relied on the use of rectangular *rf* pulses applied in the center of the nitrogen spectrum to excite heteronuclear multiple-quantum coherences comprising ^{14}N SQ or DQ transitions and to reconvert these coherences back into observable SQ coherences of the spy nuclei. The duration τ_p of the rectangular excitation and reconversion pulses applied to ^{14}N can be adjusted empirically, typically in the range $0.3\ \tau_{rot} < \tau_p < 0.6\ \tau_{rot}$. The overall efficiency of the two-way 'in-and-out' coherence transfer process is

* Corresponding author. Fax: +41 21 6933604.
E-mail address: marcanthony.caporini@epfl.ch (M.A. Caporini).

1090-7807/$ - see front matter © 2011 Elsevier Inc. All rights reserved.
doi:10.1016/j.jmr.2011.06.013

rather modest (on the order of 10%) and depends critically on the optimization of these pulses [2].

In this publication, it is shown that the efficiency can be greatly improved by replacing the long rectangular excitation and reconversion pulses at the beginning and end of the evolution interval t_1 by rotor-synchronized DANTE sequences. Typically, one may use as many as 13 short pulses in $k = 13$ rotor periods for both excitation and reconversion periods. These periods are thus much longer than the rectangular excitation and reconversion pulses that were used hitherto in our indirect detection experiments, thus taking a toll in signal intensity. Both excitation and reconversion periods can be shortened by using 'overtone' DANTE schemes comprising $n = 2$, 4 or 8 pulses per rotor period. This allows one to obtain much quicker and more efficient broadband excitation, typically in $k = 2$–4 rotor periods τ_{rot}. (Note that our use of the expression 'overtone DANTE' should not be confused with 'overtone NMR', where double-quantum transitions are excited by an *rf* field at twice the Larmor frequency [16].) To limit signal decay due to dipolar interactions, DANTE experiments are best carried out at very high spinning frequencies where the rotor periods τ_{rot} are shortest. The resulting DANTE and overtone DANTE sequences show improved excitation/reconversion efficiency, especially for large quadrupolar coupling constants, and a relatively uniform, broadband excitation profile with respect to the center of the quadrupolar powder spectra.

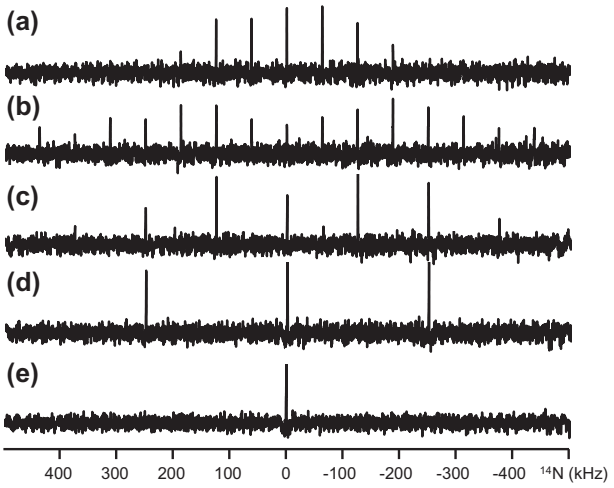

Fig. 2. Direct excitation and observation of ^{14}N magnetization in polycrystalline glycine spinning at $\nu_{rot} = 62.5$ kHz (rotation period $\tau_{rot} = 16$ μs). (a) A single rectangular pulse of duration $\tau_p = 3.5$ μs and *rf* amplitude $\omega_1(^{14}N)/(2\pi) = 60$ kHz was used for excitation. (b) Direct excitation with a basic DANTE scheme with $n = 1$ pulse per rotor period and $k = 13$ rotor periods with pulses of $\tau_p = 0.5$ μs duration each in a total time $13\tau_{rot} = 208$ μs. (c–e) Direct excitation with overtone DANTE sequences with $n = 2$ (c), 4 (d), and 8 (e) pulses per rotor period τ_{rot}. These result in inceasingly sparse sidebands that coincide with the Fourier components of the DANTE sequences at $\nu = \nu_{rf} \pm n\nu_{rot}$ (as if the effective spinning frequency were multiplied by a factor n). For (c) $\tau_p = 1.5$ μs and $k = 2$, (d) $\tau_p = 1.3$ μs and $k = 2$, and (e) $\tau_p = 0.7$ μs and $k = 2$.

2. Results and discussion

Fig. 1 depicts the pulse sequences used for direct excitation by DANTE or by a single rectangular pulse. The basic rotor-synchronized DANTE sequence has $n = 1$ pulse per rotor period as shown in Fig. 1b. Typically, the optimal excitation times for the DANTE sequence can be quite long (e.g., $k\tau_{rot} = 13\tau_{rot}$). Overtone DANTE sequences have $n = 2$, 4, or 8 pulses per rotor period and require smaller numbers of rotor periods to achieve optimal excitation (typically $2\tau_{rot} \leqslant k\tau_{rot} \leqslant 4\tau_{rot}$). In each case, the duration τ_p of the individual pulses and the number k of rotor periods are optimized to give spectra such as shown in Fig. 2. The improvements are striking. A nominal $\pi/2$ pulse merely excites sidebands across a width of ~400 kHz, with amplitudes falling off sharply at the edges. However, the DANTE pulse train excites sidebands over the entire bandwidth of the probe and produces a sideband pattern that reflects the entire breadth of the quadrupolar lineshape. As the duration τ_p of the individual pulses is increased for a fixed number of rotor periods, the response to the DANTE train is similar to a nutation experiment with very intense *rf* pulses. Overtone DANTE sequences with $n = 2$, 4, and 8 pulses per rotor period lead to spectra where, in addition to the centerband that coincides with the carrier frequency, only spinning sidebands spaced at $\pm n\nu_{rot}$ (where $n = 2$, 4, and 8) appear. Inspection of FIDs excited by overtone sequences vs signals excited by a single pulse or by a basic DANTE sequence with $n = 1$ show that the magnetization is refocused at

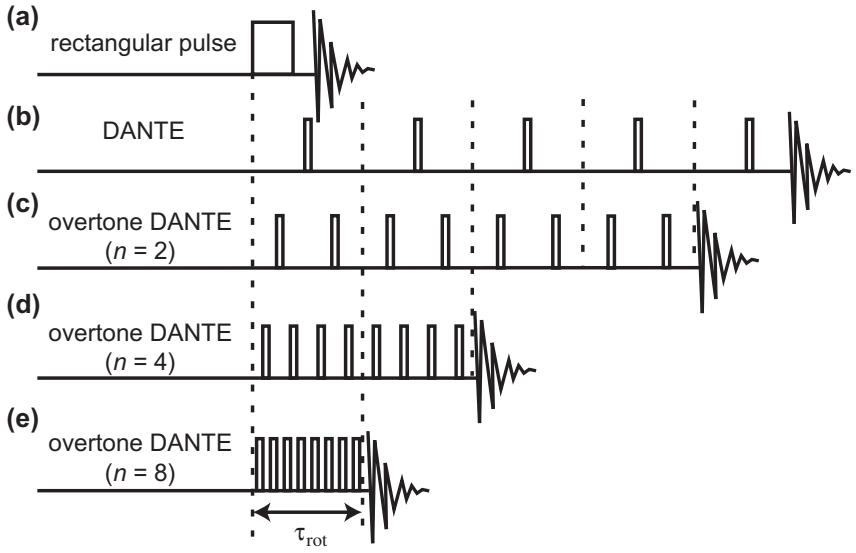

Fig. 1. Schemes illustrating the use of rotor-synchronized basic DANTE and overtone DANTE pulses. (a) A rectangular pulse with a typical duration $0.3\ \tau_{rot} < \tau_p < 0.6\ \tau_{rot}$. (b) A basic DANTE sequence with $n = 1$ pulse per rotor period. (c–e) Overtone DANTE sequences with $n = 2$, 4, and 8 pulses per rotor period.

intervals τ_{rot}/n, while ordinary rotational echoes (in the absence of *rf* pulses) occur at intervals τ_{rot}.

Overtone DANTE sequences lead to closely spaced rotational echoes and hence to sparse sideband patterns (Fig. 2) that are similar to what would be expected if the spinning frequency could be boosted by a factor n. This allows one to oversample in the t_1 dimension of a 2D indirect detection experiment by using smaller increments $\Delta t_1 = \tau_{rot}/n$. Fig. 3 compares projections onto the ^{14}N axis of D-HMQC spectra obtained with rectangular pulses and with overtone DANTE sequence with $n = 4$. The t_1 dimension was sampled in increments $\Delta t_1 = \tau_{rot}$, $\tau_{rot}/2$ and $\tau_{rot}/4$ while the total experimental time was kept constant by using the same number of scans (32) and t_1 increments (256). It should be noted that in Fig. 3d the ^{14}N signal intensity is split between the peak near the carrier and a second peak approximately $2\nu_{rot}$ downfield. Further investigations of overtone DANTE sequences are under way to explain this phenomenon.

Many solid-state NMR spectrometers are not designed to deliver sub-microsecond pulses. In practice, the rising and falling edges of the pulse shapes will be distorted, *inter alia* because of the high quality factors of the probes. Fortunately, it turns out that our DANTE sequences are quite forgiving, provided the pulse durations τ_p are longer than ~0.3 μs. Comparing to standard rectangular pulses, DANTE sequences are much less sensitive to an offset between the *rf* carrier and the center of the quadrupolar doublet. This is demonstrated in Fig. 4 where the *rf* carrier frequency $\nu_{offset}(^{14}N)$ was incremented. Shown are the projections of the signal intensity after excitation and reconversion in D-HMQC as a function of offset. While the response to a standard rectangular pulse shows a relatively high amplitude on resonance with wings on either side, the DANTE sequence and especially the overtone DANTE sequences provide a broad and relatively flat profile. The width of these profiles is limited by the Q factor of the probe.

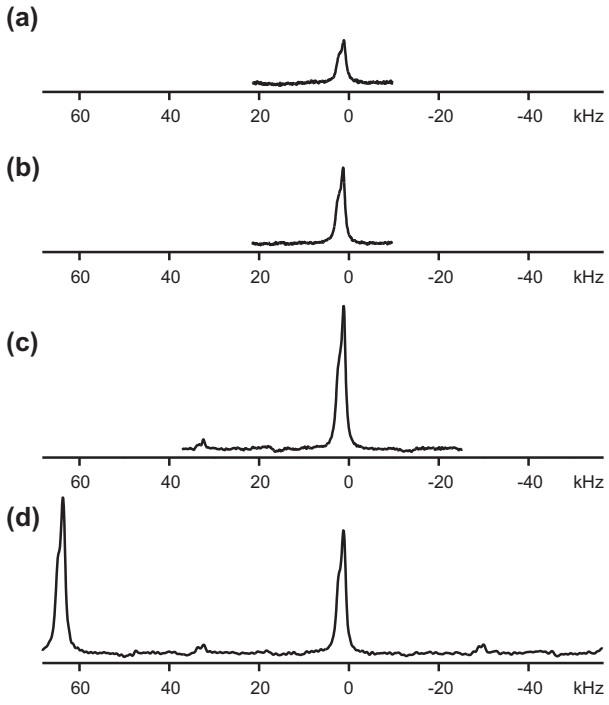

Fig. 3. Cross-sections taken along the indirect ω_1 dimension (^{14}N) of 2D spectra of glycine, spinning at $\nu_{rot} = 31.25$ kHz in a static field of 18.8 T (800 MHz for protons) using the overtone DANTE D-HMQC sequence with $n = 4$ pulses per rotor period. (a) Conventional D-HMQC sequence with $\omega_1(^{14}N)/(2\pi) = 60$ kHz and rectangular pulses $\tau_p = 18.3$ μs with increments $\Delta t_1 = \tau_{rot}$ in the indirect dimension. (b–d) Overtone DANTE D-HMQC sequence with $n = 4$ pulses per rotor period, $\tau_p = 1.6$ μs, and $k = 2$ with increments in the indirect dimension $\Delta t_1 = \tau_{rot}$ (b), ½ τ_{rot} (c), and ¼ τ_{rot} (d).

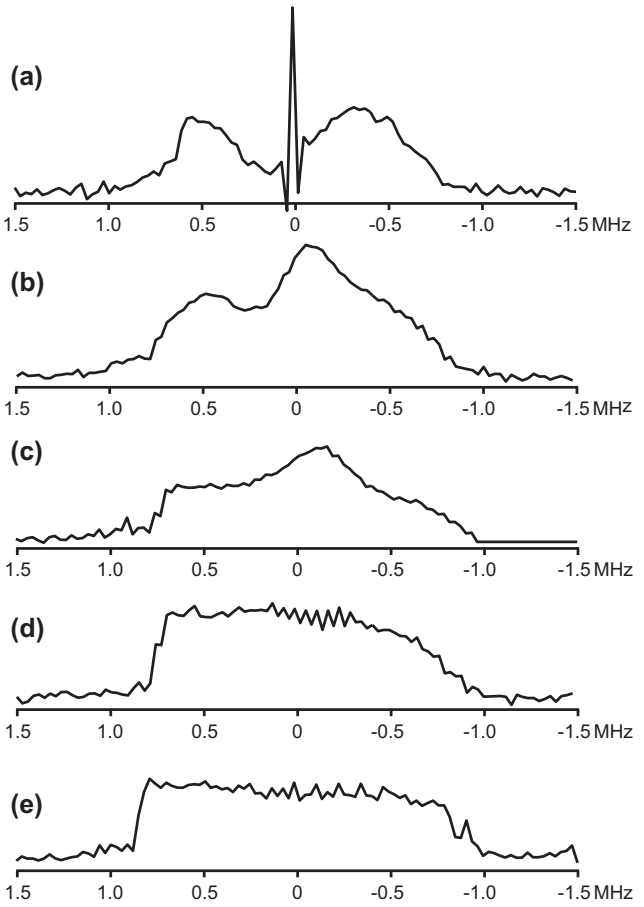

Fig. 4. Offset profiles obtained by shifting the carrier $\nu_{offset}(^{14}N)$ in steps of ν_{rot} with respect to the center of the ^{14}N quadrupolar doublets for various 2D D-HMQC sequences at $\nu_{rot} = 31.25$ kHz. (a) Conventional D-HMQC with rectangular pulses $\tau_p = 18.3$ μs. (b) Basic DANTE with $n = 1$, $k = 2$, $\tau_p = 2$ μs. (c) Overtone DANTE with $n = 2$, $k = 2$, $\tau_p = 1.5$ μs. (d) Overtone DANTE with $n = 4$, $k = 2$, $\tau_p = 1.3$ μs. (e) Overtone DANTE with $n = 8$, $k = 2$, $\tau_p = 0.9$ μs.

Further evidence of the broadband nature of DANTE and overtone DANTE sequences is demonstrated by the spectra of histidine spinning at $\nu_{rot} = 62.5$ kHz shown in Figs. 5 and 6. All ^{1}H–^{14}N correlations in the overtone DANTE D-HMQC in Fig. 5b have much greater cross-peak intensities than the standard D-HMQC of Fig. 5a, which is only effective at exciting coherences for 2 of the 3 nitrogen sites in histidine. For glycine, which has a small quadrupole interaction $C_Q = 1.18$ MHz, the efficiency of the basic DANTE sequence is comparable to a D-HMQC sequence with rectangular pulses when spinning at $\nu_{rot} = 62.5$ kHz. But for the aromatic nitrogen nuclei in histidine, which have larger quadrupolar coupling constants (up to $C_Q \sim 3$ MHz) and different isotropic chemical shifts and/or second-order quadrupole shifts, one notices a significant improvement with DANTE (Figs. 5 and 6). All three nitrogen sites in histidine N^a (= NH_3^+), N^b (= acidic aromatic NH), and N^c (= basic aromatic N) could be excited and resolved simultaneously in the indirect dimension, while in the conventional HMQC spectrum only the N^a resonance, which has the smallest quadrupole interaction and is nearest to the carrier frequency, could be excited. The improvement is illustrated in Fig. 6 by comparing cross-sections through the 2D spectra obtained with standard, DANTE, and overtone DANTE D-HMQC sequences. Note the dramatic improvement for the aromatic N^bH and N^c sites, which have larger quadrupolar coupling constants and greater offsets than N^aH_3. The best

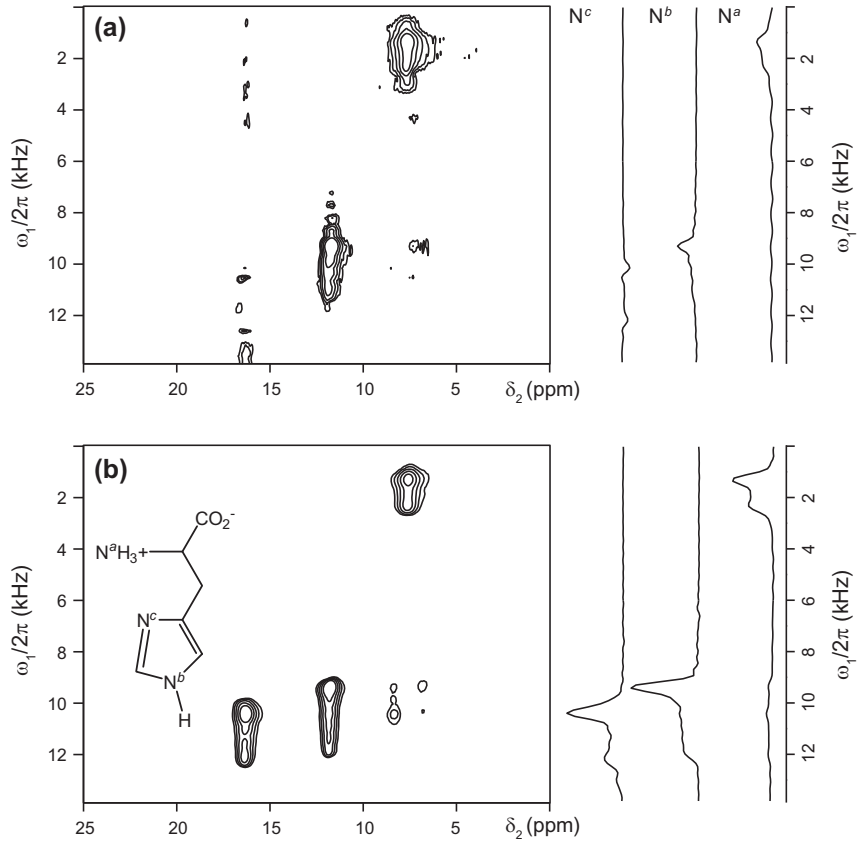

Fig. 5. Two-dimensional (2D) spectra of polycrystalline histidine spinning at ν_{rot} = 62.5 kHz in a static field of 18.8 T (800 MHz for protons), showing correlations of single-quantum (SQ) ^{14}N signals with those of neighboring protons. (a) Conventional D-HMQC sequence using rectangular pulses with $\omega_1(^{14}N)/(2\pi)$ = 60 kHz and τ_p = 11 μs. (b) Overtone DANTE D-HMQC sequence with n = 2, k = 2 and τ_p = 1.1 μs. Both spectra were recorded with 32 scans per t_1 point with 256 t_1 increments and a recycle delay of 6 s.

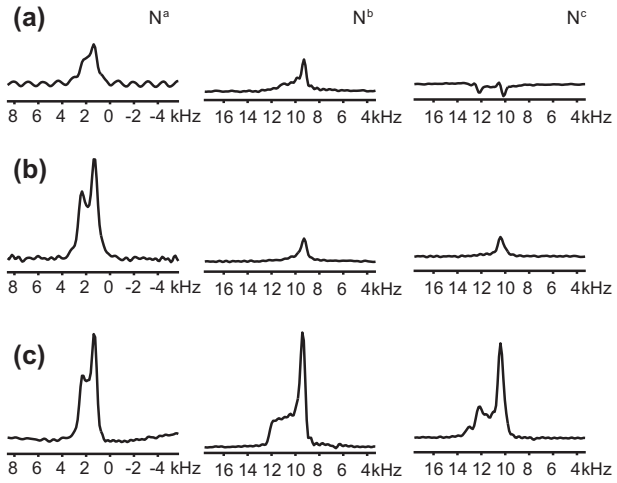

Fig. 6. Projections of cross-peaks taken from the 2D D-HMQC spectra such as those of Fig. 5 parallel to the ω_1 axis of the signals of nuclei N^a, N^b, and N^c in histidine. (a) Conventional D-HMQC sequence of Fig. 5a. (b) Basic DANTE sequence with 8 pulses of τ_p = 0.7 μs each in 8 τ_{rot} = 128 μs. (c) Overtone DANTE sequence (Fig. 5b) with 4 pulses of τ_p = 1.1 μs each in 2 τ_{rot} = 32 μs.

excitation is obtained by using an overtone DANTE sequence with n = 2 pulses per rotor period and k = 2 rotor periods, with 4 pulses of duration τ_p = 1.1 μs each, both for excitation and reconversion. The spectra in Fig. 5 and 6 also indicate that DANTE and overtone DANTE sequences can excite a range of isotropic shifts spanning at least 10 kHz. Using a basic rotor-synchronized DANTE scheme (n = 1 pulse per rotor period, k = 8 rotor periods), the spectra of Fig. 6 show that the gain in the excitation efficiency is sufficient to compensate for the T_2' losses arising from ^{1}H homonuclear dipolar couplings during as many as k = 8 rotor periods. Clearly, it is of advantage to spin the sample at high speeds to reduce the losses in the two protracted intervals $k\tau_{rot}$.

We also simulated experiments by assuming initial states $T^S_{1,1}T^I_{1,0}$ (Fig. 7a and c) or $T^S_{1,1}T^I_{2,0}$ (Fig. 7b and d) directly preceding the ^{14}N pulses. In real experiments, the expectation values of $T^I_{1,0}$ and $T^I_{2,0}$ depend on the duration τ_{exc} of the excitation delay and on the mechanisms that are acting during this interval [2,15]. We simulated DANTE sequences comprising $1 < k < 15$ rotor periods, and varied the duration of the DANTE pulses in the range $0.2 < \tau_p < 15$ μs, neglecting relaxation and broadening by dipolar interactions. The best performance was obtained with k = 12 which is quite close to the best experimental value of k = 13. After a first excitation sequence, the system was allowed to evolve in the absence of any *rf* irradiation for one rotor period. Heteronuclear coherences $T^S_{1,m}T^I_{1,\pm1}$ and $T^S_{1,m}T^I_{2,\pm1}$ were projected to simulate the effect of phase cycles. A second DANTE sequence was then simulated to reconvert the heteronuclear coherences back into the initial operators $T^S_{1,1}T^I_{1,0}$ or $T^S_{1,1}T^I_{2,0}$ for detection. In our simulations we assumed ν_{rot} = 62.5 kHz, i.e., a rotor period τ_{rot} = 16 μs, a quadrupole coupling constant C_Q = 1.18 MHz and asymmetry parameter η = 0.50, both typical for glycine, and ^{14}N–^{1}H dipolar and scalar coupling constants of 5 kHz and 65 Hz, respectively. We simulated the 'overtone' DANTE sequences in a similar manner but with n = 2 pulses per rotor period and k = 2 rotor periods, which are shown in Fig. 7c and d. The effect on the efficiency of the pulse duration τ_p and the number of rotor periods k is similar in simulations and experiments.

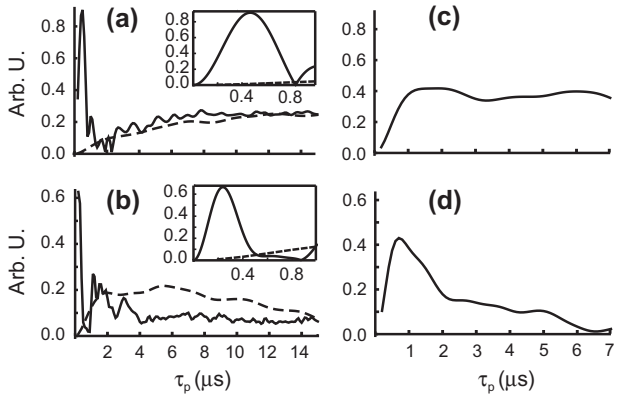

Fig. 7. (a and b) Simulations comparing the excitation/reconversion efficiency of the conventional D-HMQC vs DANTE D-HMQC for $T^S_{1,1}T^I_{1,0}$ (a) and $T^S_{1,1}T^I_{2,0}$ (b) coherences with insets highlighting short pulse duration τ_p. The DANTE versions (solid lines) with $k = 12$, $n = 1$, are plotted as a function of τ_p and compared to a single rectangular pulse (dashed lines). (c and d) Simulations of the excitation/reconversion efficiency of the $T^S_{1,1}T^I_{1,0}$ (c) and $T^S_{1,1}T^I_{2,0}$ (d) coherences for an overtone DANTE sequence with $k = 2$, $n = 2$, as a function of τ_p.

We should add a few miscellaneous observations to highlight the differences between standard pulses vs basic DANTE and overtone DANTE sequences. When optimizing the ^1H–^{14}N recoupling time using $SR4^2_1$ we often find different optimum values for standard pulses and DANTE sequences. This is most likely due to the varying efficiencies of the ^{14}N pulses in manipulating coherences of the type $T^S_{1,1}T^I_{1,0}$ vs $T^S_{1,1}T^I_{2,0}$ and the ratio between these two states after $SR4^2_1$ recoupling periods. We believe that DANTE sequences allow one to excite a larger number of crystallite orientations in a more uniform manner whereas the rectangular pulses select a much smaller subset of crystallite orientations. To clarify these points, more simulations need to be carried out.

3. Conclusions

It has been shown that there are considerable advantages in replacing rectangular excitation pulses by rotor-synchronized DANTE sequences. This can be beneficial both for direct excitation of ^{14}N spectra and for indirect detection via spy nuclei such as ^1H or ^{13}C. To limit signal decay due to dipolar interactions, DANTE experiments are best carried out at very high spinning frequencies.

The basic and overtone DANTE schemes presented here may be broadly applicable to many systems under MAS where the breadth of the spectrum is many times larger than both the MAS frequency and the available *rf* field strength. For half-integer quadrupolar nuclei this may significantly improve the excitation and detection of satellite transitions. These methods may also be useful for spin 1/2 nuclei if spinning is slow or the *rf* field strength low, or if anisotropic interactions such as hyperfine couplings are much larger than the spinning frequency and the *rf* field strength. This may be especially relevant for paramagnetic systems used in some dynamic nuclear polarization (DNP) experiments. Rotor synchronized microwave pulses might also be useful for manipulating coherences in electron spin resonance and for DNP.

4. Experimental

Experiments at $\nu_{rot} = 62.5$ kHz were carried out in the NMR facility at the University of Lille in a static magnetic field of 18.8 T (800 MHz for protons) using a Bruker Avance III spectrometer equipped with a 1.3 mm MAS HX probe. Experiments at $\nu_{rot} = 31.25$ kHz were performed at EPFL at 18.8 T with a Bruker Avance II spectrometer equipped with a 2.5 mm MAS HXY probe. On both spectrometers the ^{14}N *rf* field strength was calibrated to 60 kHz using NH_4Cl for all ^{14}N pulses. The proton *rf* fields were typically set to the highest available field strength (100 kHz or more) for the $\pi/2$ and π pulses of D-HMQC experiments and calibrated appropriately for $SR4^2_1$ recoupling at the two MAS frequencies. To test the experiments, we used polycrystalline glycine, which has a quadrupole coupling constant $C_Q = 1.18$ MHz and an asymmetry parameter $\eta = 0.5$, and histidine, which has three distinct quadrupole coupling constants in the range 1–3 MHz [17]. Protons were used as spy nuclei for the indirect detection of nitrogen-14 by D-HMQC [8–15]. Initially, we replaced each rectangular nitrogen-14 pulse by a DANTE sequence, lasting $11 < k < 13$ rotor periods with a single pulse per rotor period ($n = 1$), with pulse durations $\tau_p \sim 0.7$ μs or shorter. The excitation and reconversion DANTE sequences are symmetrical, i.e., have the same n, k and pulse duration τ_p. It is crucial that the DANTE pulses in the reconversion step occur during the exact same fraction of the rotor period as in the excitation step. We optimized the efficiency of the scheme by varying both the number k of rotor periods and the duration τ_p of the individual pulses. Similarly, overtone DANTE sequences with $n = 2$, 4, or 8 pulses per rotor period were optimized by varying the number $2 \leqslant k \leqslant 4$ of rotor periods and the pulse durations $\tau_p \sim 1$ μs.

For direct excitation and detection of ^{14}N, the receiver bandwidth was set to 1 MHz and the ^{14}N *rf* field strength was calibrated to 60 kHz using NH_4Cl. For direct excitation of ^{14}N, we used DANTE and overtone DANTE sequences that had previously been optimized for indirect detection. A recycle delay of 3 s and 128 scans were used for the spectra in Fig. 2.

The offset profiles were recorded by applying D-HMQC sequences with either rectangular pulses or DANTE sequences to glycine and varying the offset of the carrier frequency $\nu_{offset}(^{14}N)$ in the range $-1.5625 < \nu_{offset}(^{14}N) < +1.5625$ MHz in steps of ν_{rot}.

Simulations were carried out to compare the efficiency of DANTE sequences and rectangular pulses for the excitation and reconversion pulses used for the indirect detection of nitrogen-14. We assumed a proton-detected D-HMQC scheme. Our custom Matlab code included the effects of first- and second-order heteronuclear *I–S* dipolar interactions, quadrupole interactions up to third order and scalar couplings. Second-order dipole–quadrupole cross terms (i.e., residual dipolar splittings) were also included.

Acknowledgments

The kind support of Dr. Julien Trébosc, Dr. Olivier Lafon, and Prof. Dr. Jean-Paul Amoureux at the facility in Lille is gratefully acknowledged. This work was supported by the Swiss National Science Foundation (FNS) and the Swiss Commission for Technology and Innovation (CTI), and by the *Fédération de Recherche* (FR3050) *Très Grands Equipements de Résonance Magnétique Nucléaire à Très Hauts Champs* (TGE RMN THC) of the French CNRS.

References

[1] T. Giavani, H. Bildsoe, J. Skibsted, H.J. Jakobsen, ^{14}N MAS NMR spectroscopy and quadrupole coupling data in characterization of the IV ↔ III phase transition in ammonium nitrate, J. Phys. Chem. B 106 (2002) 3026–3032.
[2] S. Cavadini, S. Antonijevic, A. Lupulescu, G. Bodenhausen, Indirect detection of nitrogen-14 in solid-state NMR spectroscopy, ChemPhysChem 8 (2007) 1363–1364.
[3] G. Bodenhausen, R. Freeman, G.A. Morris, A simple pulse sequence for selective excitation in Fourier transform NMR, J. Magn. Reson. 23 (1976) 171–175.
[4] G.A. Morris, R. Freeman, Selective excitation in Fourier transform nuclear magnetic resonance, J. Magn. Reson. 29 (1978) 433–462.
[5] P. Caravatti, G. Bodenhausen, R.R. Ernst, Selective pulse experiments in high-resolution solid state NMR, J. Magn. Reson. 55 (1983) 88–103.

[6] D.E. Wemmer, E.K. Wolff, M. Mehring, Multiple-frequency excitation (MFE) a technique for observing broadline transients, J. Magn. Reson. 42 (1981) 460–473.
[7] L.A. O'Dell, R.W. Schurko, QCPMG using adiabatic pulses for faster acquisition of ultra-wideline NMR spectra, Chem. Phys. Lett. 464 (2008) 97–102.
[8] Z. Gan, Measuring amide nitrogen quadrupolar coupling by high-resolution $^{14}N/^{13}C$ NMR correlation under magic-angle spinning, J. Am. Chem. Soc. 128 (2006) 6040–6041.
[9] S. Cavadini, A. Lupulescu, S. Antonijevic, G. Bodenhausen, Nitrogen-14 NMR spectroscopy using residual dipolar splittings in solids, J. Am. Chem. Soc. 128 (2006) 7706–7707.
[10] S. Cavadini, S. Antonijevic, A. Lupulescu, G. Bodenhausen, Indirect detection of nitrogen-14 in solids via protons by nuclear magnetic resonance spectroscopy, J. Magn. Reson. 182 (2006) 168–172.
[11] S. Cavadini, Indirect detection of nitrogen-14 in solid-state NMR spectroscopy, Prog. Nucl. Magn. Reson. Spectrosc. 56 (2010) 46–77.
[12] Z. Gan, J.P. Amoureux, J. Trébosc, Proton detected ^{14}N MAS NMR using homonuclear decoupled rotary resonance, Chem. Phys. Lett. 435 (2007) 163–169.
[13] S. Cavadini, A. Abraham, G. Bodenhausen, Proton-detected nitrogen-14 NMR by recoupling of heteronuclear dipolar interactions using symmetry-based sequences, Chem. Phys. Lett. 445 (2007) 1–5.
[14] O. Lafon, Q. Wang, B. Hu, F. Vasconcelos, J. Trébosc, S. Cristol, F. Deng, J.P. Amoureux, Indirect detection via spin-1/2 nuclei in solid state NMR spectroscopy: application to the observation of proximities between protons and quadrupolar nuclei, J. Phys. Chem. A 113 (2009) 12864–12878.
[15] S. Cavadini, V. Vitzthum, S. Ulzega, A. Abraham, G. Bodenhausen, Line-narrowing in proton-detected nitrogen-14 NMR, J. Magn. Reson. 202 (2010) 57–63.
[16] R. Tycko, S.J. Opella, Overtone NMR spectroscopy, J. Chem. Phys. 86 (1987) 1761.
[17] M.J. Hunt, A.L. Mackay, D.T. Edmonds, Nuclear quadrupole resonance of ^{14}N in imidazole and related compounds, Chem. Phys. Lett. 34 (1975) 473–475.